Vibrational Analysis of TeCl$_4$. II. A Hartree–Fock, MP2, and Density Functional Study

ATTILA KOVÁCS,[1] GÁBOR I. CSONKA[2]

[1] Research Group for Technical Analytical Chemistry of the Hungarian Academy of Sciences at the Institute of General and Analytical Chemistry of the Budapest Technical University, H-1521 Budapest, Hungary
[2] Department of Inorganic Chemistry of the Budapest Technical University, H-1521 Budapest, Hungary

ABSTRACT: The geometry and vibrational spectrum of TeCl$_4$ was calculated with various quantum chemical methods [Hartree–Fock, second-order Møller-Plesset (MP2) and generalized gradient approximation density functional theory (GGA-DFT)]. Five different basis-set combinations were tested: the relativistic effective core potentials with double-zeta split valence basis (RECP) of Hay & Wadt (HW) and Stevens et al. (CEP); the above RECP basis sets extended with polarization functions for Te and using a 6-31G* basis for Cl (HW* and CEP*); a medium-size all-electron basis set (ALL). The quality of the calculated data was assessed by comparison with recent experimental results. The Hartree-Fock method combined with the HW and CEP basis sets provided a very good approximation of the experimental vibrational spectra. The quality of the results is comparable to those of the best methods (MP2, B3-P, B3-PW with HW* and CEP* and B3-LYP, B3-P, B3-PW with the ALL basis set). However, the HW and CEP basis sets provided very poor geometry and vibrational frequencies when they were used in combination with any correlated method in this work. Similarly, the DFT methods using Becke's 1988 exchange functional (B-LYP, B-P, B-PW) without the inclusion of the exact exchange let to very poor results with the basis sets used in this study.   © 1997 John Wiley & Sons, Inc. Int J Quant Chem **65**: 817–826, 1997

Introduction

Vibrational data are of great importance at various fields of chemistry and physics such as molecular mechanics and molecular dynamics, statistical thermodynamics, gas electron diffraction analysis, etc. However, their experimental determination for inorganic molecules is difficult. High temperatures, long path lengths, and sensitive detectors are needed to detect the (often low-intense) vibrational bands of the low-volatile compounds. Additionally, the interpretation of the high-temperature spectra is hampered by the broad rotational contours, hot bands, and possible presence of other components in the gas phase (decomposition and association products). Hence, results from other techniques such as matrix isolation spectroscopy and theoretical methods are acknowledged to extend the high-temperature experimental data.

The quantum chemical calculations have been successfully applied for the interpretation and prediction of vibrational spectra of organic compounds [1]. However, the application for inorganic molecules is more difficult. First of all, these latter molecules are usually built up out of heavier elements, rendering the computations with all-electron basis sets very expensive. Furthermore, the errors arising from the neglect of relativistic effects are important from the fourth row of the periodic table. These two problems can be solved by using relativistic effective core potentials (RECP) [2–8], which are extensively used in Hartree-Fock (HF) and post-HF calculations.

The density functional (DFT) methods are known to provide good estimates of the vibrational spectra of organic compounds. Recent DFT studies of transition-metal complexes also have shown promising agreement with the experimental infrared (IR) frequencies and intensities [9, 10]. However less information is available about the performance of the DFT methods with effective core potentials. The use of DFT functionals with ECPs generated previously from Hartree–Fock atomic calculations is not free of problems. Since the exchange and correlational functionals are nonlinear in the density, the core and valence densities are not strictly separable. Hence, the use of ECPs generated from HF calculations should be carefully tested for their applicability in DFT work. Promising results have been published recently by

Russo et al. [11]. Investigating a small but representative set of transition-metal compounds [ScF_3, TiF_4, VF_5, TiO, $Ni(CO)_4$, CuF], they found that the RECPs of Hay and Wadt [2–4] can be used in DFT methods, as well.

In the present study we test the performance of currently most successful generalized gradient approximation (GGA) and hybrid DFT methods using effective core potentials as compared to Hartree−Fock and second-order Møller-Plesset (MP2) methods as well as to all-electron basis sets.

The tellurium tetrachloride molecule was chosen as a model for this study. Its molecular geometry (determined by gas electron diffraction) and experimental vibrational spectra are known from a recent study [12]. The $TeCl_4$ molecule has a trigonal bipyramid structure with a vacant equatorial position (C_{2v} symmetry). The molecular geometry is in accordance with the valence-shell electron-pair repulsion (VSEPR) theory [13]. Characteristics are the axial Te—Cl bonds being longer than the equatorial bonds and the axial chlorines being slightly bent toward the equatorial ones. Concerning the vibrational data, eight of the nine fundamentals of $TeCl_4$ were found in the experimental specta and a good estimate [based on a scaled quantum mechanical (SQM) [14] force field] is available for the unobserved A_2 (ν_4) mode [12].

Computational Details

Geometries, Cartesian harmonic force constants, and IR intensities of $TeCl_4$ were calculated at the HF, MP2 [15], and DFT levels of theory using the Gaussian 94 program [16]. Six exchange-correlation density functionals were employed in the present study: Becke's 1988 (B) [17] and Becke's three parameter (B3) [18] gradient-corrected exchange functionals were combined with the Lee−Yang−Parr (LYP) [19], Perdew (P) [20], and Perdew−Wang (PW) [21] correlation functionals. The default grid (75,302) implemented in the Gaussian 94 program was used in the DFT calculations. We used five different basis set combinations:

1. **HW:** the Hay & Wadt RECPs with double-zeta valence basis sets for both Cl and Te [3]
2. **CEP:** the RECPs of Stevens et al. and the corresponding double-zeta valence basis sets for both Cl and Te [5, 6]
3. **HW*:** the 6-31G(d) basis set for chlorine and the Hay & Wadt RECP with double-zeta va-

lence basis set [3] extended with a single set of *d*-type polarization functions [22] for tellurium

4. CEP*: the 6-31G(d) basis set for chlorine and the RECP of Stevens et al. with double-zeta valence basis set [6] extended with a single set of *d*-type polarization functions [22] for tellurium

5. ALL (all-electron basis set): the standard 6-31G(d) basis set for chlorine and a 3-21G(d) basis [23] for tellurium

Harmonic vibrational frequencies and IR intensities were computed for the fully optimized geometries. The first derivatives of the potential energy with respect to the nuclear coordinates were calculated analytically at all quantum chemical levels. The second derivatives were obtained analytically for the all-electron basis set and numerically for the RECP basis sets.

Results and Discussion

GEOMETRY

The computed geometrical parameters of $TeCl_4$ obtained at various levels of theory are compared to the experimental geometry in Table I.

The DFT methods containing Becke's 1988 exchange functional (B-LYP, B-P, and B-PW) with the most economic HW and CEP basis sets found the T_d geometry as a single minimum on the *potential energy surface*. All the other calculations converged to the right C_{2v} structure resulting longer axial Te—Cl bonds with respect to the equatorial ones in accordance with the experimental data. The methods resulting in false geometries were omitted from the further studies.

Figures 1(a) and 1(b) show the deviations between the calculated and experimental geometrical parameters. The most significant difference between the computed results is the very poor performance of the HW and CEP basis sets for bond distances [cf. Fig. 1(a)].

The calculated bond lengths are longer than the experimental ones, with one exception of the HF/HW* result for the Te—Cl_{eq} bond. In general, the computations underestimate the Cl_{eq}—Te—Cl_{eq} bond angle, however, differ in the character of the Cl_{ax}—Te—Cl_{eq} angle (cf. Table I). The experimental tilt of the axial chlorines toward the equatorial ones is reproduced by the HF and MP2 methods (except the MP2/CEP level) and by the

B3-type DFT/ALL calculations. In all the other cases no tilt, or a small opposite tilt, was obtained. The latter bond angle is generally overestimated by the various methods, except the HF with all the basis sets and the MP2/ALL [cf. Fig. 1(b)]. The deviations for all the geometrical parameters are generally larger than the experimental errors.

In general, the computed bond lengths and the Cl_{ax}—Te—Cl_{eq} angle increase in the order HF < MP2 < B3-P ∼ B3-PW < B3-LYP < B-P ∼ B-PW < B-LYP. [The only significant deviation from this trend was found for the bond lengths obtained at the MP2/HW and CEP levels; cf. Fig. 1(a)]. We note that similar behavior has been found earlier for C—C and C—O bond lengths of sugars and 1,2-ethanediol [24, 25]. The computed Cl_{eq}—Te—Cl_{eq} bond angle varies in a narrower range. The above trend, but with negative sign (because of the underestimating character of the computations), can be recognized, except for the results obtained by using the ALL basis set.

Summing up, the experimental geometry of $TeCl_4$ is best reproduced by the HF and MP2 methods. The DFT methods provided poorer results, especially those that contain the B-type exchange functional. The HW*, CEP*, and ALL basis sets are of similar quality, HW* being slightly superior; the HW and CEP basis sets are much poorer.

FREQUENCIES

The observed and computed fundamentals of $TeCl_4$ are compiled in Table II. The deviations between selected computed and the experimental frequencies are shown in Figure 2. We present here the results obtained at various levels of theory using the HW and HW* basis sets. They resemble the results obtained with the other related basis sets (HW to CEP, HW* to CEP* and ALL). The following trend can be observed: The B3-type DFT/HW and B-type DFT/HW* frequencies are considerably underestimated, while the HF and MP2/HW* ones are overestimated. The HF/HW and most of the B3-type DFT/HW* frequencies vary around the experimental values. We note the significant underestimation of the ν_8 and ν_9 stretching fundamentals by the DFT calculations. The computed frequencies increase in the order B-LYP < B-P ∼ B-PW < B3-LYP < B3-PW ∼ B3-P < MP2 < HF. This trend is just the opposite to that seen for most of the geometrical parameters (cf. Fig. 1).

TABLE I
Molecular geometry of TeCl₄.

Basis[a]	Method	Bond length (Å)		Bond angle (deg)		
		Te — Cl$_{ax}$	Te — Cl$_{eq}$	Cl$_{ax}$ — Te — Cl$_{ax}$	Cl$_{eq}$ — Te — Cl$_{eq}$	Cl$_{ax}$ — Te — Cl$_{eq}$
	Exp.[b]	2.430(6)	2.298(6)	175.9(6)	103.0(7)	88.7[c]
HW	HF	2.537	2.409	172.8	101.4	87.7
	MP2	2.588	2.468	177.8	100.5	89.3
	B-LYP[d]	2.585		109.5		
	B-P[d]	2.568		109.5		
	B-PW[d]	2.566		109.5		
	B3-LYP	2.578	2.481	174.3	99.3	91.9
	B3-P	2.559	2.463	176.6	99.6	90.9
	B3-PW	2.560	2.466	177.6	99.9	90.8
CEP	HF	2.568	2.431	174.4	100.6	88.2
	MP2	2.626	2.501	177.9	98.6	90.7
	B-LYP[d]	2.607		109.5		
	B-P[d]	2.587		109.5		
	B-PW[d]	2.586		109.5		
	B3-LYP	2.600	2.505	171.0	98.7	92.9
	B3-P	2.579	2.486	174.8	99.2	91.7
	B3-PW	2.583	2.491	173.9	99.1	92.0
HW*	HF	2.440	2.290	175.2	100.7	88.1
	MP2	2.441	2.313	176.6	100.2	88.9
	B-LYP	2.507	2.389	172.5	99.4	92.4
	B-P	2.485	2.369	174.6	99.5	91.7
	B-PW	2.479	2.367	175.9	100.0	91.3
	B3-LYP	2.472	2.346	179.0	100.1	90.4
	B3-P	2.453	2.330	179.6	100.2	89.9
	B3-PW	2.455	2.333	179.8	100.1	89.9
CEP*	HF	2.461	2.313	175.5	100.6	88.5
	MP2	2.463	2.339	176.8	100.4	89.0
	B-LYP	2.522	2.415	172.2	99.9	92.5
	B-P	2.500	2.395	174.9	100.1	91.6
	B-PW	2.499	2.393	174.9	100.1	91.7
	B3-LYP	2.491	2.371	178.8	100.2	90.4
	B3-P	2.471	2.354	179.7	100.3	89.9
	B3-PW	2.475	2.357	179.8	100.3	90.1
ALL	HF	2.449	2.317	173.5	100.7	87.9
	MP2	2.448	2.338	174.7	100.5	88.3
	B-LYP	2.509	2.410	178.5	102.3	90.4
	B-P	2.481	2.383	179.6	102.2	89.9
	B-PW	2.480	2.382	179.8	102.1	89.9
	B3-LYP	2.477	2.368	177.8	101.7	89.3
	B3-P	2.452	2.345	176.8	101.5	89.0
	B3-PW	2.456	2.348	176.9	101.5	89.0

[a] For details of basis sets HW, CEP, HW*, CEP*, and ALL see text.
[b] From a gas electron diffraction study, Ref. [12], r_a values.
[c] Calculated from the data given in Ref. [12].
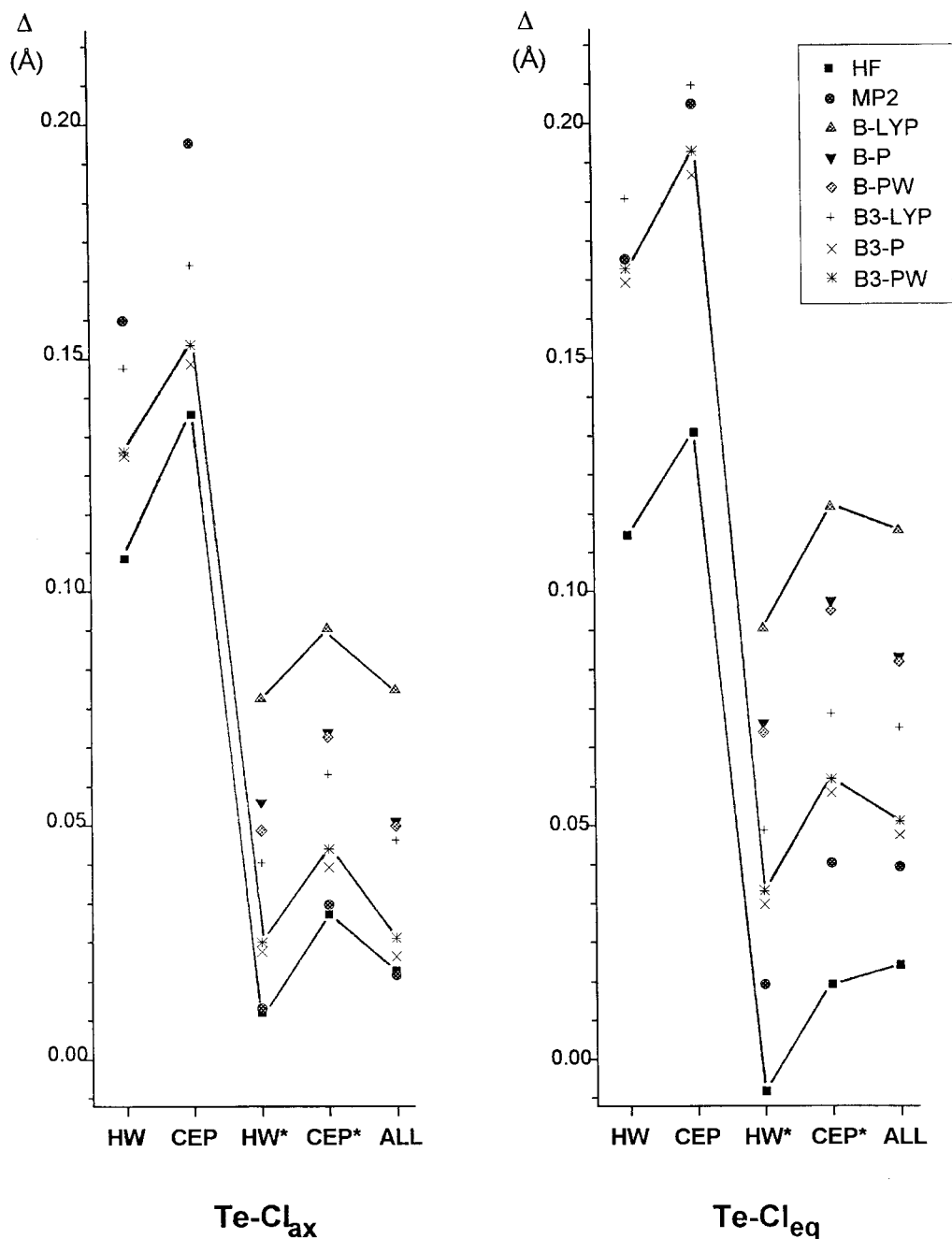[d] The computed geometry has tetrahedral symmetry.

FIGURE 1a. Deviations between computed and experimental geometrical parameters: (a) bond lengths; (b) bond angles.

The performance* of the computational levels can be assessed and compared by the root-mean-square (rms) and maximal deviations between the

*By performance we mean here how the different theoretical levels are able to estimate the experimental (anharmonic) vibrational spectra. We do not intend to investigate the quality of the calculated harmonic frequencies.

experimental and theoretical frequencies (Fig. 3).[†] The rms deviations are scattered within the 8–53 cm^{-1} range, while the maximal deviations (absolute values) vary from 15 to 80 cm^{-1}.

[†] The ν_4 mode was not involved in the evaluation of these deviations.
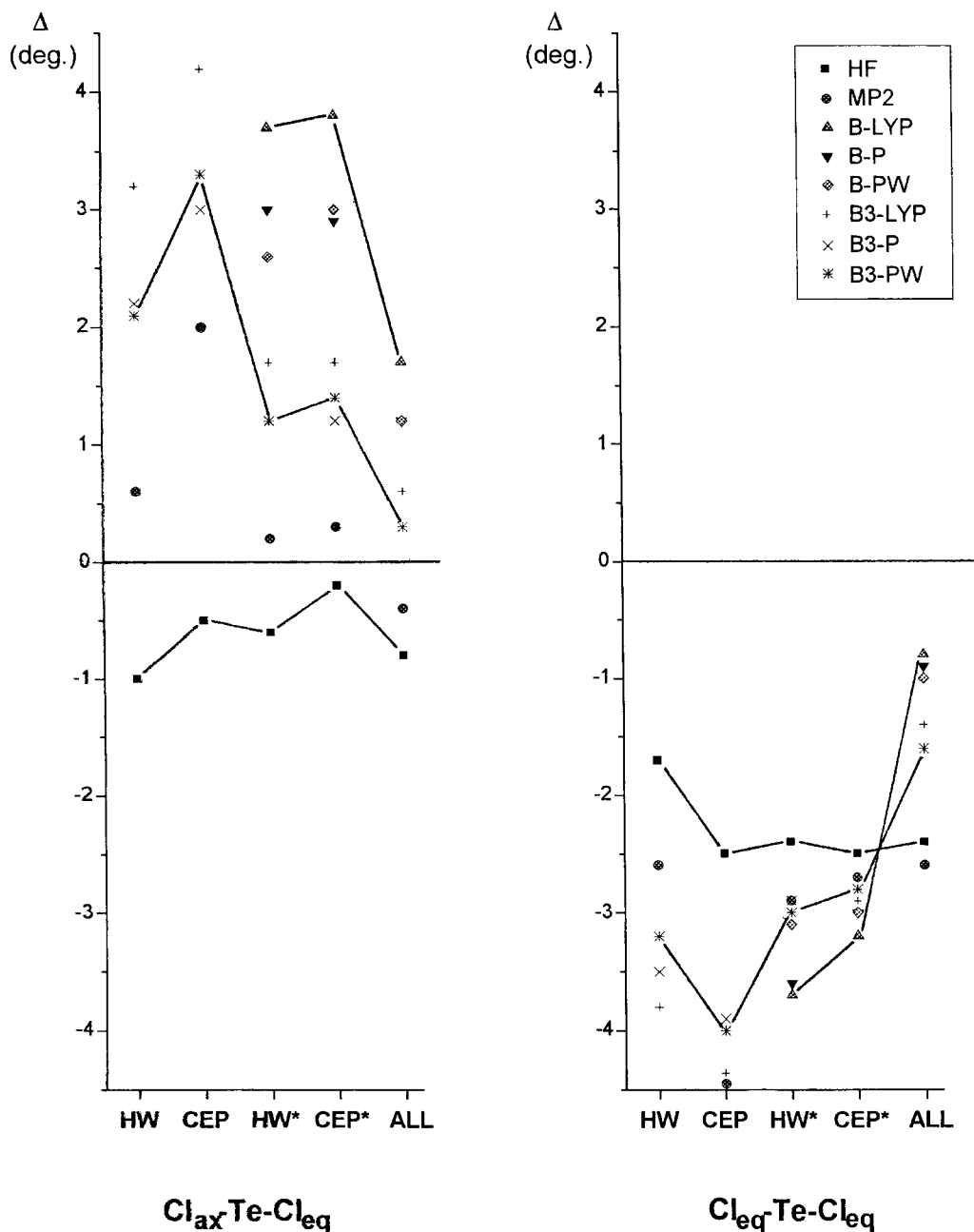
FIGURE 1b. (continued)

On Figure 3 a significant trend can be observed for both the theoretical levels and the basis sets, a trend which is reflected at both the rms and maximal deviations.

The performance of the HW and CEP basis sets used with the correlated methods is very poor, however, it is surprisingly good with the Hartree-Fock theory. The HF/HW level belongs even to the best methods. The HW*, CEP*, and ALL basis sets performed well with the MP2 and B3-type DFT levels, while about two–three times larger deviations can be observed for the results obtained at the B-type DFT calculations. It is noteworthy that the MP2/HW* and CEP* frequencies are in very good agreement with the experimental data, however, the agreement worsened using the all-electron (ALL) basis set. Here the B3-type DFT levels are definitely superior. We note also the

TABLE II
**Experimental and calculated fundamentals (cm^{-1}) and calculated IR intensities (km mol^{-1}) of TeCl$_4$.**

Basis[a]	Method	ν_1	ν_2	ν_3	ν_4	ν_5	ν_6	ν_7	ν_8	ν_9	rms dev.	max. dev.
	Exp.[b]	72	104	158	(150[c] ± 10)	165	290	312	378	382		
HW	HF	73 (3)	107 (13)	150 (19)	160 (0)	174 (8)	285 (1)	307 (224)	366 (21)	359 (9)	10.5	21
	MP2	57 (3)	82 (9)	125 (11)	133 (0)	147 (4)	254 (1)	299 (145)	319 (24)	315 (10)	38.0	67
	B3-LYP	50 (3)	61 (6)	109 (6)	113 (0)	128 (2)	258 (4)	300 (129)	308 (33)	309 (14)	46.8	73
	B3-P	52 (2)	67 (6)	133 (7)	118 (0)	133 (2)	265 (4)	309 (134)	320 (34)	321 (15)	37.3	61
	B3-PW	53 (2)	68 (6)	111 (7)	121 (0)	135 (3)	266 (4)	310 (133)	316 (35)	318 (13)	40.8	64
CEP	HF	73 (4)	102 (13)	147 (18)	153 (0)	168 (6)	271 (1)	300 (279)	365 (22)	354 (11)	15.4	28
	MP2	54 (4)	69 (8)	117 (8)	121 (0)	135 (2)	238 (2)	294 (162)	303 (29)	306 (14)	48.2	76
	B3-LYP	40 (3)	54 (5)	103 (4)	108 (0)	123 (1)	250 (6)	300 (154)	298 (38)	306 (16)	52.7	80
	B3-P	48 (3)	63 (6)	108 (6)	115 (0)	130 (2)	258 (6)	310 (161)	309 (41)	317 (16)	44.7	69
	B3-PW	47 (3)	61 (6)	107 (6)	115 (0)	130 (2)	257 (6)	308 (160)	307 (40)	315 (16)	46.0	71
HW*	HF	96 (3)	128 (10)	181 (14)	184 (0)	201 (10)	301 (2)	306 (341)	408 (60)	415 (23)	25.3	36
	MP2[b]	85 (2)	113 (7)	163 (9)	166 (0)	183 (5)	291 (3)	322 (256)	376 (59)	385 (21)	9.4	18
	B-LYP	65 (2)	72 (4)	126 (4)	127 (0)	146 (1)	258 (8)	290 (186)	315 (62)	326 (22)	37.2	63
	B-P	67 (2)	79 (4)	131 (5)	134 (0)	153 (1)	270 (7)	303 (194)	331 (64)	341 (23)	27.1	47
	B-PW	70 (1)	86 (4)	132 (5)	137 (0)	155 (2)	271 (7)	305 (196)	330 (64)	342 (22)	26.0	48
	B3-LYP	72 (2)	95 (5)	145 (7)	149 (0)	167 (2)	275 (5)	305 (229)	345 (62)	357 (22)	16.7	33
	B3-P	73 (2)	100 (6)	149 (7)	154 (0)	172 (3)	286 (5)	317 (234)	358 (65)	370 (22)	9.6	20
	B3-PW	78 (2)	100 (6)	150 (7)	153 (0)	171 (3)	284 (5)	315 (234)	357 (64)	369 (22)	10.0	21
CEP*	HF	92 (3)	122 (9)	177 (15)	176 (0)	195 (8)	304 (2)	314 (353)	400 (61)	407 (25)	20.3	30
	MP2	80 (2)	107 (7)	158 (10)	158 (0)	175 (5)	291 (3)	328 (256)	368 (59)	376 (22)	8.4	16
	B-LYP	59 (2)	73 (3)	118 (4)	122 (0)	139 (1)	262 (8)	299 (183)	309 (60)	320 (22)	40.3	69
	B-P	64 (2)	79 (4)	124 (5)	128 (0)	146 (2)	273 (8)	312 (194)	325 (64)	335 (22)	30.6	53
	B-PW	64 (2)	80 (4)	126 (5)	130 (0)	147 (2)	273 (8)	312 (196)	326 (64)	336 (22)	29.8	52
	B3-LYP	72 (2)	92 (5)	141 (7)	142 (0)	160 (2)	277 (6)	313 (229)	340 (62)	352 (22)	19.3	38
	B3-P	74 (2)	96 (5)	145 (8)	147 (0)	164 (3)	288 (5)	324 (237)	354 (65)	365 (23)	12.5	24
	B3-PW	74 (2)	95 (5)	145 (8)	146 (0)	164 (3)	286 (6)	322 (237)	352 (65)	363 (23)	13.3	26
ALL	HF	96 (2)	131 (8)	181 (13)	183 (0)	200 (11)	307 (2)	327 (326)	411 (64)	416 (26)	27.0	35
	MP2	86 (1)	119 (6)	166 (9)	167 (0)	184 (6)	299 (3)	341 (252)	384 (62)	389 (23)	15.2	29
	B-LYP	52 (2)	80 (4)	125 (5)	138 (0)	155 (1)	238 (3)	267 (197)	335 (65)	338 (23)	36.5	52
	B-P	64 (1)	95 (4)	135 (5)	147 (0)	164 (2)	266 (4)	301 (205)	353 (67)	355 (23)	18.5	27
	B-PW	73 (1)	99 (4)	139 (5)	142 (0)	157 (3)	279 (6)	321 (207)	341 (68)	348 (23)	19.9	37
	B3-LYP	70 (2)	104 (5)	146 (7)	155 (0)	172 (3)	275 (4)	309 (233)	365 (66)	369 (23)	9.8	15
	B3-P	74 (1)	111 (5)	152 (7)	161 (0)	177 (4)	294 (4)	332 (239)	380 (68)	384 (24)	9.1	20
	B3-PW	79 (1)	112 (5)	154 (7)	156 (0)	171 (5)	293 (4)	333 (238)	364 (68)	375 (24)	10.4	21

[a] For details of basis sets HW, CEP, HW*, CEP*, and ALL see text.
[b] From Ref. [12].
[c] SQM value using the MP2/HW* harmonic force field.

significant improvement of the results obtained at the B3-LYP level used with the ALL basis set compared to those with HW* and CEP*. The results of the B3-P and B3-PW levels used with CEP* worsened somewhat compared to those using the HW* basis and to MP2/CEP*. The performance of the Hartree–Fock theory with these three larger basis sets is similar to that of the B-type DFT methods.

The best agreement between the experimental and computed frequencies was obtained at the MP2/CEP* level, however, only slightly worse are the HF/HW, the MP2, B3-P and B3-PW/HW*, and the B3-P, B3-LYP and B3-PW/ALL results (rms deviation less than 11 cm^{-1}, maximal deviation not exceeding 21 cm^{-1}).

The computed vibrational data of TeCl$_4$ are suitable to assist the assignment of the bands in
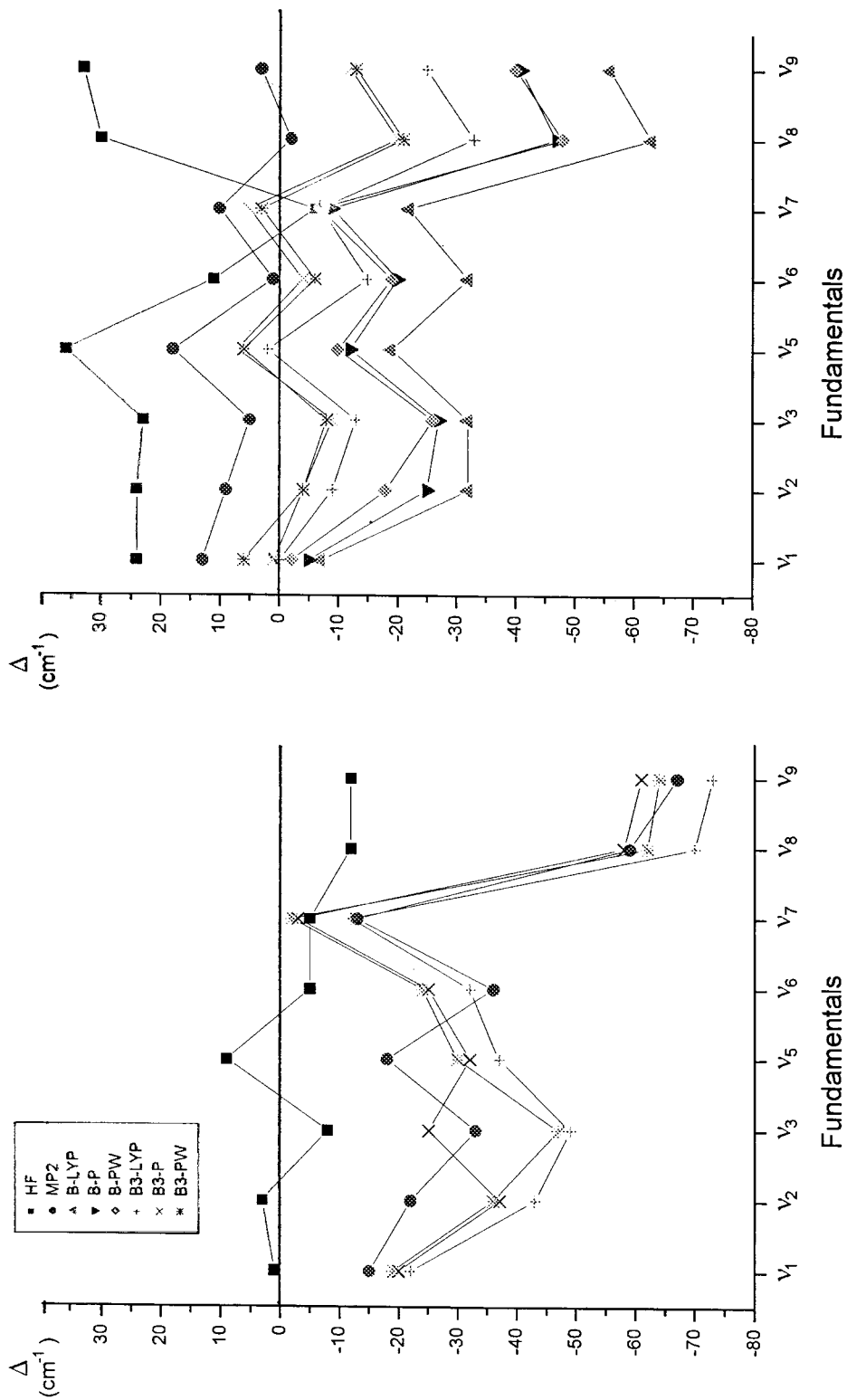
FIGURE 2. Deviations between calculated and experimental vibrational frequencies obtained at various levels of theory using basis sets (a) HW and (b) HW*.
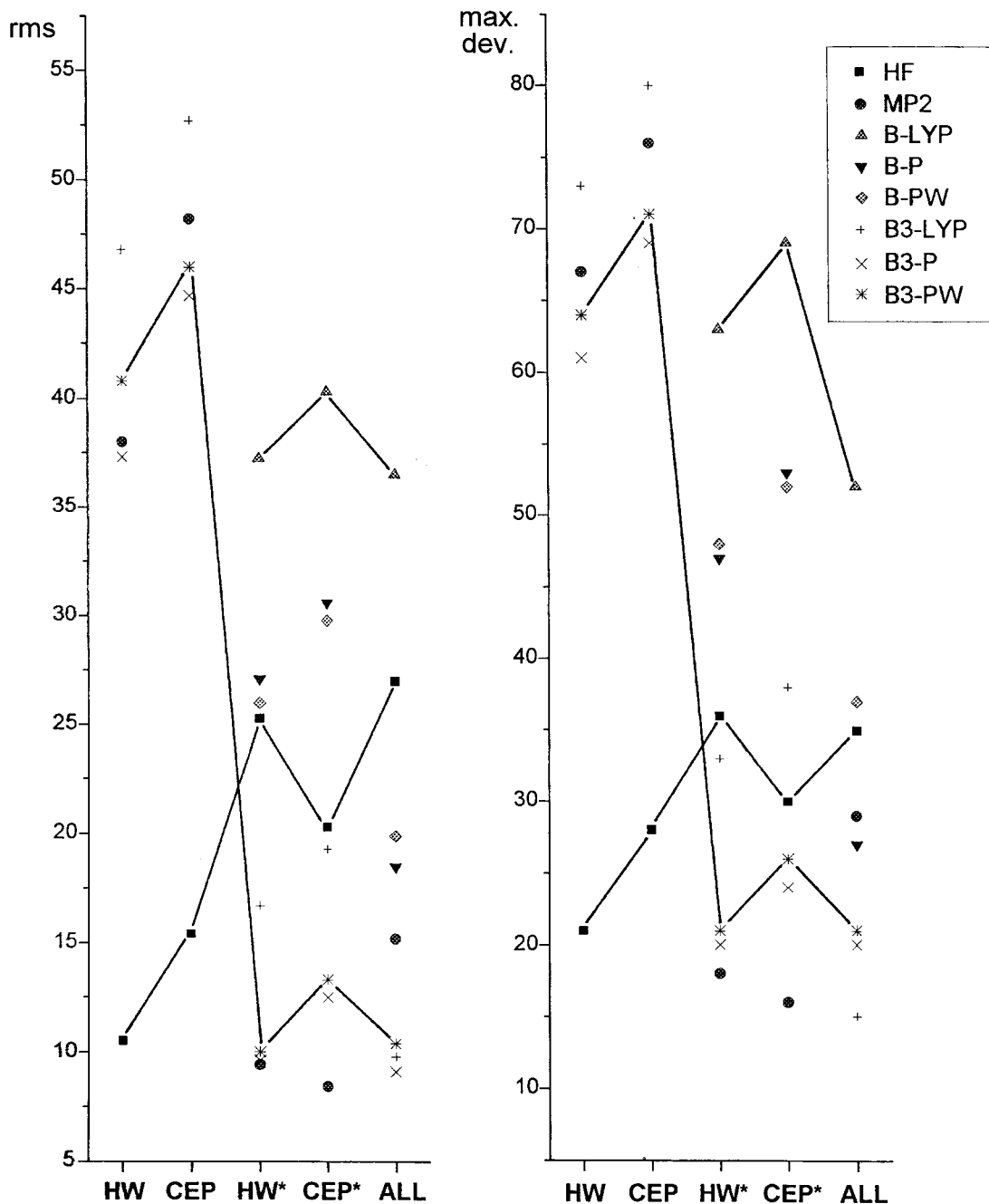
FIGURE 3. (a) Rms and (b) maximal deviations (absolute values) between the calculated and experimental vibrational frequencies.

the experimental spectra (cf. Table II). The stretching fundamentals can be assigned unambiguously by the computed IR intensities. In most cases the relative sequence of the frequencies is in accord with the experimental observations, and only the computed ν_8 and ν_9 stretching fundamentals are interchanged at the HF/HW, HF/CEP, and MP2/HW levels as well as the calculated ν_7 and ν_8 modes at the B3-P and B3-PW/CEP levels. The deformation modes have similar (small) computed

IR intensities, and the relative order of their frequencies agrees with that of the experimental ones. The unobserved ν_4 mode was positioned between ν_3 and ν_5 by all the quantum chemical calculations except for B3-P/HW and HF/CEP*, however the experimental values of these fundamentals are also very close [12].

Conclusions

1. The molecular geometry of $TeCl_4$ is best reproduced at the HF and MP2 levels using the HW*, CEP*, and ALL basis sets. The density functional methods gave rise to poorer results, especially those using Becke's 1988 exchange functional. The RECP basis sets (HW and CEP) provided poor results, especially for the bond distances.

2. Generally, the vibrational frequencies calculated by the MP2 and B3-type DFT methods with basis sets HW*, CEP*, and ALL (except MP2/ALL and B3-LYP/HW* and CEP*) as well as at the HF/HW level are in good accord with the experimental data. The agreement is good enough to assist the assignment of the measured vibrational spectra.

3. The HW and CEP basis sets compensate effectively the errors of the HF method for $TeCl_4$. The HW* and CEP* basis sets are best combined with MP2, B3-P and B3-PW. Regarding the all-electron basis set a combination with the B3-type DFT methods is superior.

4. Based on their performance and cost effectiveness the methods using relativistic effective core potentials are advantageous for large-scale computations.

References

1. B. A. Hess, Jr., J. Schaad, P. Cársky, and R. Zahradník, Chem. Rev. **86**, 709 (1986).
2. P. J. Hay and W. R. Wadt, J. Chem. Phys. **82**, 270 (1985).
3. W. R. Wadt and P. J. Hay, J. Chem. Phys. **82**, 284 (1985).
4. P. J. Hay and W. R. Wadt, J. Chem. Phys. **82**, 299 (1985).
5. W. J. Stevens, H. Basch, and M. Krauss, J. Chem. Phys. **81**, 6026 (1984).
6. W. J. Stevens, M. Krauss, H. Basch, and P. G. Jasien, Can. J. Chem. **70**, 612 (1992).
7. L. F. Pacios and P. A. Christiansen, J. Chem. Phys. **82**, 2664 (1985).
8. M. M. Hurley, L. F. Pacios, P. A. Christiansen, R. B. Ross, and W. C. Ermler, J. Chem. Phys. **84**, 6840 (1986).
9. L. Fan and T. Ziegler, J. Phys. Chem. **96**, 6937 (1992).
10. R. Fournier and I. Pápai, in *Recent Advances in Density Functional Methods, Part 1.*, D. Chong, Ed. (World Scientific, Singapore, 1995).
11. T. V. Russo, R. L. Martin, and P. J. Hay, J. Phys. Chem. **99**, 17085 (1995).
12. A. Kovács, K.-G. Martinsen, and R. J. M. Konings, J. Chem. Soc. Dalton Trans., 1037 (1997).
13. R. J. Gillespie and I. Hargittai, *The VSEPR Model of Molecular Geometry* (Allyn and Bacon, Boston, 1991).
14. P. Pulay, G. Fogarasi, G. Pongor, J. E. Boggs, and A. Vargha, J. Am. Chem. Soc. **105**, 7073 (1983).
15. C. Møller and M. S. Plesset, Phys. Rev. **46**, 618 (1934).
16. M. J. Frisch, G. W. Trucks, H. B. Schlegel, P. M. W. Gill, B. G. Johnson, M. A. Robb, J. R. Cheeseman, T. Keith, G. A. Petersson, J. A. Montgomery, K. Raghavachari, M. A. Al-Laham, V. G. Zakrezewski, J. V. Ortiz, J. B. Foresman, J. Cioslowski, B. B. Stefanov, A. Nanayakkara, M. Challacombe, C. Y. Peng, P. Y. Ayala, W. Chen, M. W. Wong, J. L. Andres, E. S. Replogle, R. Gomperts, R. L. Martin, D. J. Fox, J. S. Binkley, D. J. DeFrees, J. Baker, J. J. P. Stewart, M. Head-Gordon, C. Gonzalez, and J. A. Pople, Gaussian 94, Revision B.2, Gaussian, Inc., Pittsburgh, PA, 1995.
17. A. D. Becke, Phys. Rev. A **38**, 3098 (1988).
18. A. D. Becke, J. Chem. Phys. **98**, 5648 (1993).
19. C. Lee, W. Yang, and R. G. Parr, Phys. Rev. B **37**, 785 (1988).
20. J. P. Perdew, Phys. Rev. B **33**, 8822 (1986).
21. J. P. Perdew and Y. Wang, Phys. Rev. B **45**, 13244 (1992).
22. B. A. Smart and C. H. Schiesser, J. Comp. Chem. **16**, 1055 (1995).
23. K. D. Dobbs and W. J. Hehre, J. Comp. Chem. **7**, 359 (1986).
24. G. I. Csonka and I. G. Csizmadia, Chem. Phys. Lett. **243**, 419 (1995).
25. G. I. Csonka, K. Éliás, and I. G. Csizmadia, Chem. Phys. Lett. **257**, 49 (1996).